High Harmonic Generation Spectra of Neutral Helium by the Complex-Scaled (t,t') Method: Role of Dynamical Electron Correlation

Nimrod Moiseyev* and Frank Weinhold

Department of Chemistry and Minerva Center of Nonlinear Physics in Complex Systems, Technion-Israel Institute of Technology, Haifa 32000, Israel

and Theoretical Chemistry Institute and Department of Chemistry, University of Wisconsin, Madison, Wisconsin 53706

(Received 5 August 1996)

Using highly correlated Hylleraas-type wave functions of ^1S and ^1P symmetry, we show how the harmonic generation spectrum of $1\,^1S$ He (including short wavelength members previously attributed to He^+) arise from a radial-angular "descreening" mechanism. This provides the first indication that harmonic generation spectrum can arise from strong dynamical electron correlations rather than purely as a "one-electron phenomenon." [S0031-9007(97)02676-8]

PACS numbers: 42.65.Ky

Interest in tunable short-wavelength sources has stimulated numerous experimental and theoretical investigations of harmonic generation spectra (HGS) of noble gases in intense laser fields [1]. Using an ultra-high-power KrF laser (5 eV photons), Sarukura *et al.* [2] found the relative intensities of 9th to 23rd-order harmonics of helium from a single-shot experiment with peak intensity of 2×10^{17} W/cm^2. From the dependence of calculated neutral atom and ion responses on field intensity [see Fig. (5) in Ref. [3]], one can judge that below 3.2×10^{15} W/cm^2 the field is below saturation intensity, whereas fields exceeding 10^{16} W/cm^2 are above it. The 3.5×10^{16} W/cm^2 can be regarded as the field intensity where the transition from neutral He to He^+ occurs. Although at this intensity 100% of helium is ionized after the end of the laser pulse ($\sim$120 cycles), only 50% of helium atoms are ionized when the laser pulse reaches 0.905 of its maximal value (after $\sim$55 cycles). Indeed, the best fit to the experimental HGS was obtained for intensities near 3.5×10^{15} W/cm^2.

Previous theoretical fits to the experimental spectrum have involved two distinct models. Fits up to the 13th harmonic order were achieved for neutral helium atoms described by a one-electron "frozen orbital" model Hamiltonian or by Hartree-Fock (HF) or density functional methods [3–5]. In such approximations, dynamical electronic correlations are ignored entirely (frozen orbital, HF) or treated in the framework of the homogeneous electron gas (in which, e.g., the strong "radial" or "angular" correlations of inhomogeneous atomic systems have no direct counterpart). The fit to higher harmonics, on the other hand, was achieved with a He^+ model [4,5]. These combined fitting procedures have led to common interpretation of HGS as a "one-electron phenomenon" [4,5].

The present work employs highly accurate Hylleraas-type wave functions with much greater variational flexibility to correctly describe the dynamical radial and angular correlation effects in ground and excited resonance states of helium atoms. Many years ago, it was shown by Moiseyev and Katriel [6] that coupling of radial and angular correlations can actually lead to the electrons being drawn closer together, rather than pushed apart, toward the low-Z end of the helium isoelectronic sequence. We have previously described the critical role of such radial and angular correlations in enhancing the lifetime of helium autoionizing states [7]. The simple physical picture underlying such coupling effects can be sketched as follows: In atoms, the dominant correlating motions in the $1/Z$ perturbation expansion are of radial ("in-out") and angular type. The former cause the electrons to separate into inner and outer orbits, while the latter keep the electrons on opposite sides of the nucleus. The effect of the third-order coupling of radial and angular correlations is then to bring the electrons back closer together, since the outer most electron will now "see" the other electron tending to lie *behind* the nucleus, thus "descreening" the nuclear charge. This confers some He^+-like character on the inner part of the wave function, permitting the outer electron to move closer to the nucleus and to reduce the radial separation that was established in lower order. Although initially drawn for field-free resonances, this picture of dynamical correlations also has obvious relevance for helium in intense laser fields. Of course, we do not employ perturbative approximations in our actual calculations, but we emphasize that the variational treatment must have sufficient flexibility to correctly incorporate the physical correlation effects that appear in low perturbative order. For this purpose, the Hylleraas-type wave functions (with explicit incorporation of interelectron distance r_{12}) are unmatched accuracy and utility.

The fact that only odd-order harmonics were observed in the HGS experiments, even when the atoms were exposed to short laser pulses, is an indication that the dynamics of the helium electrons in strong fields is controlled by a *single* resonance Floquet state. Indeed, previous numerical calculations [8] have shown remarkable agreement between HGS calculated from direct solutions of the time-dependent Schrödinger equation with nonperiodic Hamiltonians and the corresponding result from Fourier analysis of the time- dependent dipole moment for a *single resonance Floquet quasienergy state*, provided the duration

 0031-9007/97/78(11)/2100(4)$10.00

of the laser pulse is larger than 15–50 oscillations of the electric field (see Fig. 7 in Ref. [8]). We therefore study the dynamics of helium in an ac field from the Floquet starting point, using the momentum gauge.

As a basis set we used the ground and lowest excited ^1S and ^1P states of field-free helium, the lowest ^1S and ^1P autoionizing resonances, and a discrete representation of the continuum which was rotated into the lower half of the complex energy plane by the complex-coordinate rotation technique [9]. The bound states, autoionizing resonances ("double excited" states), and rotating continua are all numerical eigenfunctions of the complex-scaled Hamiltonian [10]. The advantage of using the complex scaling method lies in the dramatic reduction in the number of states needed to calculate the converged resonance Floquet state. Upon complex scaling, the autoionization resonances (which are present also in the field-free spectrum) and associated Floquet quasienergy resonances are represented by *square-integrable* wave functions of pronounced bound-state character (nodal structure related to quantum number, etc.). One may say that the use of complex scaling "collects" information about the decay process from an infinite number of continuum states and "concentrates" it into a single square-integrable function. The price we pay is that the complex-scaled Hamiltonian is not Hermitian and the associated scalar product should be replaced by the more general *c*-product [11].

The bound and resonance states are localized in the potential interaction region, whereas the rotating continuum states are delocalized functions having nearly zero amplitude in this region. Therefore, only the bound (ground and excited), resonance, and *low*-lying rotating continuum states (i.e., those close to the threshold energies) will make large contributions in the basis-set expansion of the resonance Floquet wave function. These basis states were obtained by diagonalizing a complex-scaled matrix of higher order for the field-free electrostatic Hamiltonian. The Hylleraas-type "primitives" underlying this calculation are of the form $(1 + \hat{P}_{12}) r_1^l r_2^m r_{12}^k (\cos\theta_1)^\lambda \times \exp(-\beta_1 r_1 - \beta_2 r_2)$ where $\hat{P}_{12}$ permutes electron levels and the other symbols have their usual meaning [12]. This basis is in principle complete for *any* choice of the nonlinear parameters β_1, β_2 for both S states ($\lambda = 1$), provided sufficiently high integer powers of r_1, r_2, and r_{12} are included. We included all (138:95 for ^1S symmetry states and 43 for the ^1P ones) possible terms for which $l + m + k$ is less than or equal to 8, and we chose $\beta_1 = \beta_2 = 1.0$ for S states and $\beta_1 = 0.9$, $\beta_2 = 1.7$ for P states, sufficient to reproduce the known eigenvalues [13] of the ground and first 5–10 excited bound states (with zero width) to at least 10^{-5} a.u. accuracy for both symmetries. Note that 2-β corresponds approximately to the screening of one electron by the other, so that the P-type Hylleraas functions are chosen with β_{inner} for nearly a bare He^+-line charge. The leading autoionizing resonances "$(2s)^2$," "$2s2p$," ..., were obtained with comparably high accuracy for both position and lifetime.

For the time-dependent problem with external field $(\epsilon_0/\omega)(\hat{p}_1 + \hat{p}_2)\sin(\omega t)$, the Hamiltonian becomes $\mathbf{H}(t) = \mathbf{E}^d - (\epsilon_0/\omega)\mathbf{d}\sin(\omega t)$, where $\mathbf{E}^d$ is the diagonalized matrix of the time-independent, field-free system when all bound, all resonances, and the rotating continua with imaginary parts which are smaller than 0.1 eV were used as a basis set. All together, 42 ^1S and ^1P symmetry correlated eigenstates were kept for the time propagation. $\mathbf{d}$ is the matrix representation of the dipole momentum operator $\hat{p}_1 + \hat{p}_2$ (in the same basis of the field-free Hylleraas functions as $\mathbf{E}^d$). The corresponding Floquet operator is represented by the matrix $\mathcal{H}(t) = \mathbf{1}(-i\hbar\partial/\partial t) + \mathbf{H}(t)$. The (t, t') method [14,15] then enables us to describe the time evolution operator as a single exponential operator, $\mathbf{U}(t, t') = \exp[-it\mathcal{H}(t')/\hbar]$, where the physical time evolution operator is a cut in the t, t' plane, $\mathbf{U}(t, t' = t)$. The (t, t') technique can increase the speed of calculations dramatically, even by several orders of magnitude [16]. By diagonalizing the complex non-Hermitian matrix $\mathbf{U}(t, t')$, we obtain the quasienergy Floquet states Ψ_{QE} and the corresponding eigenvalues, $\Lambda = \exp(-iE_{\text{QE}}T/\hbar)$, where $T = 2\pi/\omega$ is the periodicity of the field (in our case, $\hbar\omega = 5$ eV). The free complex scaling parameter [9] was optimized to obtain stable HG spectra and not stationary values of the lifetimes of the resonance Floquet states in order to minimize the size of the basis set. Therefore the ionization rates that we calculated are not precise.

In Fig. 1 we show the squared overlap $|\langle 1\,^1S|\text{QE}\rangle|^2$ of the longest-lived resonance Floquet state ("QE") with the complex-scaled field-free $1\,^1S$ ground state as a function of field intensity I_0 (proportional to ε_0/ω^2). One can see that a sharp change in the contribution of the He

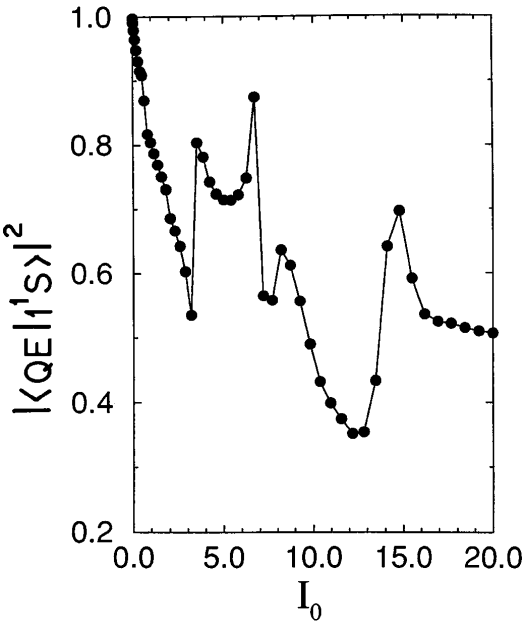

FIG. 1. Squared overlap $|\langle \text{QE}|^1S\rangle|^2$ of the longest-lived Floquet state "QE" with the complex-scaled helium $1\,^1S$ ground state as a function of field intensity $I_0 = 335.111\varepsilon_0^2$.

ground state to the resonance Floquet occurs near $I_0 = 3.5 \times 10^{15}$ W/cm^2. The abrupt change in Floquet resonance composition is due to an avoided crossing phenomenon. Figure 2 shows how the complex eigenvalue Λ of the long-lived "$1\,^1S$ resonance" (open circles, with width $\simeq$0.002 a.u. $\simeq$ 0.054 eV) moves clockwise as field intensity increases, whereas the "$2\,^1P$ resonance" (closed circles) which is dominated by the lowest excited P states, moves counterclockwise. At a very specific field intensity, these two resonance Floquet states move very close to one another in complex energy space ("crossing" on the real axis). At this point a strongly mixed configuration state is obtained, having sharply reduced $1\,^1S$ character. The situation is more complicated than depicted in Fig. 2, since other higher resonance Floquet states (associated with higher excited ^1P states) also become involved in the overlapping of multiple avoided crossings in this region.

The association of enhanced high harmonics in the HGS with field-dependent avoided crossings has been previously recognized [8]. Moreover, it was shown that plateau-type HGS is obtained when a nonlinear continuously driven system exhibits chaotic classical dynamics [17]. Marcus long ago pointed out that overlapping multiple avoided crossings provide a diagnostic fingerprint of classical chaotic dynamics [18]. Our results in Figs. 1 and 2 therefore suggest that, for a field intensity near 3.5×10^{15} W/cm^2, the overlapping of several resonance Floquet states should lead to enhanced high harmonics or even to the appearance of a "plateau"-like feature in high HGS. Indeed, that is what we have found.

Figure 3 depicts the field-dependent changes in the calculated HGS (on a logarithmic intensity plot) near the onset of the plateau-like behavior. When the results are presented on an "absolute" scale (see, e.g., Potvliege and Shakeshaft in Ref. [19]), one immediately can see that it is far from being a plateau. (After the submission of this paper Preston *et al.* [20] published new experimental data with HG spectra up to the 35th harmonic, which enable one to see the deviation from a plateau-like behavior, even on a logarithmic scale.) There is, however, a clear enhancement of the high harmonics in the harmonic generation, as expected. Whereas weaker fields give unstable HGS with exponentially diminishing intensities for higher harmonics, one sees that near 3.2×10^{15} W/cm^2 (closed circles) a highly *stable* plateau-like behavior (i.e., enhancement of the probability to observe high harmonics) begins to set in. Closer study shows that the HGS is most stable with respect to small variations in the maximum field amplitude for 3.46×10^{15} W/cm^2, in very satisfying agreement with field intensities inferred from previous "best" theoretical fits to experimental data [3]. However, whereas previous neutral helium treatments [3–5] (based on frozen orbital, HF, or density functional approximations) could fit experimental data only up to $n = 13$, our results exhibit excellent agreement with experiment for the full range of observed harmonics up to $n = 23$, as shown in Fig. 4.

All HGS were obtained by repropagating the "$1\,^1S$" resonance Floquet state [i.e., the eigenfunction $\Psi_{\mathrm{QE}}(t) = \hat{U}(t, t')\Psi_{\mathrm{QE}}(t = 0)|_{t'=t}$] of the time evolution operator $\hat{U}(t, t')$ having at least 50% contribution from the field-free He $1\,^1S$ ground state. The nth order member $(n\mu_n)$ of the HGS is obtained from the nth Fourier component (μ_n) of the time-dependent dipole expectation value $\langle\Psi_{\mathrm{QE}}(t)\,|\,\hat{p}_1 + \hat{p}_2|\Psi_{\mathrm{QE}}(t)\rangle_c$, where $\langle\ldots\rangle_c$ denotes the c-product [11]. Note that there is a simple relation between the time derivative of the dipole moment in the length gauge, $\dot{d}$, and the time-dependent dipole moment in the momentum gauge, $\dot{d} = \langle\Psi|\,\hat{p}_1 + \hat{p}_2 - (\varepsilon_0/\omega)\sin\omega t|\Psi\rangle_c$, so that the dipole acceleration is given by $\partial/\partial t\langle\Psi|\,\hat{p}_1 + \hat{p}_2|\Psi\rangle_c - \varepsilon_0\cos\omega t = \sum_n i\omega n\mu_n \exp(i\omega nt) - \varepsilon_0/2(e^{i\omega t} - e^{-i\omega t})$.

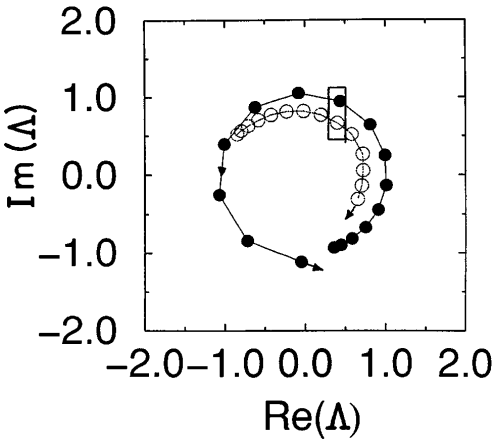

FIG. 2. Field-dependent ε_0 trajectories of complex eigenvalues of the time evolution operator, $\Lambda = \exp(-iE_{\mathrm{QE}}2\pi/\omega)$, where E_{EQ} are the complex resonance eigenvalues of the complex-scaled Floquet operator associated with the $1\,^1S$ ground state (open circles) and an excited ^1P state (filled circles), showing the near degeneracy (box) associated with onset of plateau-like HGS.

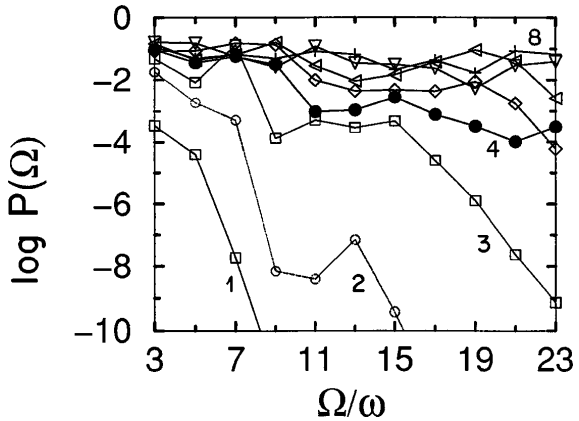

FIG. 3. Field-dependent HGS for the *single* longest-lived ("$1\,^1S$-like") resonance Floquet state, showing the onset of transition to stable plateau-like HGS near 3.2×10^{15} W/cm^2. ($I_0 = 3.2 \times 10^{15}(i/4)^2; i = 1, \ldots, 8$). The HG were scaled to make the $\Omega = 9\omega$ of the 4th spectra to coalesce with the experimental results.

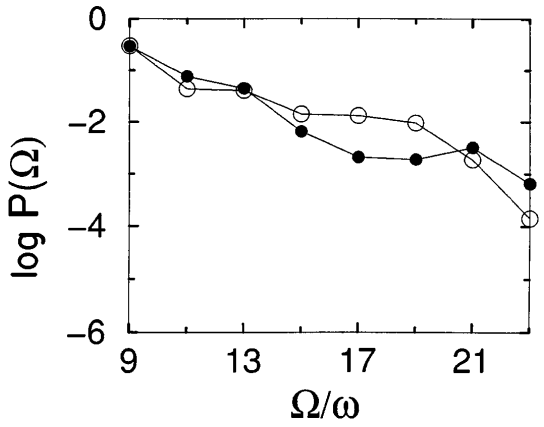

FIG. 4. Experimental HGS (filled circles, Ref. [2]) compared with present theoretical work for field intensity 3.46×10^{15} W/cm^2 (open circles).

We can obtain further insight into the role of dynamical electron correlations in generating high HGS by reducing the flexibility of the Hylleraas-type basis (e.g., omitting powers of r_{12}) to "control" the degree of correlation allowed into the description. If we first set $l = k = 0$ in all Hylleraas terms, forcing one electron to be "1s-like" in every term, the resonance Floquet state (neglecting spin dependence) is necessarily of the form $\Psi_{\mathrm{QE}}(t) = 1s(\vec{r}_1)\phi(\vec{r}_2, t) + 1s(\vec{r}_2, t)\phi(\vec{r}_1, t)$, where ϕ is a linear combination of terms $r^m \exp(-\beta t)$, $m = 0$–5. Such a function is of unrestricted Hartree-Fock (UHF) form, simulating the much lower correlation treatment of previous models [3–5]. This UHF-like model reproduces the experimental harmonics up to $n = 15$, but fails thereafter. As more terms restored to the full Hylleraas expansion (allowing more correlation flexibility) successive harmonics "pop out" to the experimentally observed plateau. Thus, we find that excellent agreement with the entire experimental high HGS up to $n = 23$ can be obtained if electron correlation effects are treated with sufficient accuracy. (Note that our results, like those of previous theoretical studies, are for an *isolated atom* exposed to an intense laser field, and therefore cannot incorporate collective effects that may be present in the experimental spectra.)

Our results may seem to contradict the theoretical results presented in Refs. [4,5], which found it necessary to employ excited He or He^+ models to reproduce higher HGS peaks. However, as pointed out above, the actual correlated behavior of the inner electron is indeed rather He^+-like, and the previous treatments of electron correlation were simply too crude to exhibit this aspect of the neutral atom directly. Moreover, it is clear that neutral He atoms must be abundantly present under the experimental conditions, since at 3.5×10^{15} W/cm^2 the density of atoms is estimated [21] to equal that of ions (10–20 torr, corresponding to about 10^{17}–10^{18} atoms/cm^3). Our results therefore support the possibility that the *entire* HGS spectrum is due to a *single* species (neutral helium), and that the higher harmonics are a result of strong two-electron correlations, rather than a "one-electron phenomenon."

In conclusion, we find that (a) HGS in He can be treated as a *single* Floquet mode phenomenon, (b) an explicit connection can be drawn between stable HGS to small variations in the field intensity and overlapping avoided crossings of resonance quasienergy states, mediated by a critical field intensity of $\sim 3.5 \times 10^{15}$ W/cm^2, and (c) strong radial-angular coupling gives rise to "correlation-induced descreening" in neutral helium that accounts for the increased He^+-like character leading to the shortest-wavelength HGS emissions.

*Electronic address: nimrod@chem.technion.ac.il

[1] A. L'Huillier, K. J. Schafer, and K. C. Kulander, Phys. Rev. Lett. **66**, 2200 (1991); A. L'Huillier and P. Balcou, Phys. Rev. Lett. **70**, 774 (1993) and references therein.
[2] N. Sarukura, K. Hata, T. Adachi, and R. Nodomi, Phys. Rev. A **43**, 1669 (1991).
[3] A. Sanpera, P. Jonsson, J. B. Watson, and K. Burnett, Phys. Rev. A **51**, 3148 (1995).
[4] Xu Huale, X. Tang, and P. Lambropoulos, Phys. Rev. A **46**, R2225 (1992).
[5] C. A. Ullrich, S. Erhard, and E. K. U. Gross, in *Super Intensity Laser Atomic Physics IV*, edited by H. G. Muller (Kluwer, Boston, 1996).
[6] N. Moiseyev and J. Katriel, Chem. Phys. **10**, 67 (1975).
[7] N. Moiseyev and F. Weinhold, Phys. Rev. A **20**, 27 (1979).
[8] N. Ben-Tal, N. Moiseyev, R. Kosloff, and C. Cerjan, J. Phys. B **26**, 1446 (1993).
[9] W. P. Reinhardt, Annu. Rev. Phys. Chem. **33**, 223 (1982); N. Moiseyev, Isr. J. Chem. **31**, 311 (1991).
[10] N. Moiseyev, P. R. Certain, and F. Weinhold, Mol. Phys. **36**, 1613 (1978).
[11] N. Moiseyev, in *Letropet Symposium View on a Generalized Inner Product*, edited by E. Brändas and N. Elander, Lecture Notes in Physics Vol. 325 (Springer-Verlag, Berlin, 1989), p. 549.
[12] E. A. Hylleraas, Adv. Quantum Chem. **1**, 1 (1964).
[13] C. L. Pekeris, Phys. Rev. **126**, 143 (1968).
[14] U. Peskin and N. Moiseyev, J. Chem. Phys. **99**, 4590 (1993).
[15] N. Moiseyev, Comments At. Mol. Phys. **31**, 88 (1995).
[16] U. Peskin, R. Kosloff, and N. Moiseyev, J. Phys. Chem. **100**, 8849 (1994).
[17] V. Averbukh and N. Moiseyev, Phys. Rev. A **51**, 3911 (1995).
[18] R. A. Marcus, in *Quantum Chaos*, edited by G. Cassati and J. Ford (Academic, New York, 1984).
[19] P. M. Potvliege and R. Shakeshaft, Phys. Rev. A **40**, 3061 (1989).
[20] S. G. Preston, A. Sanpera, M. Zept, W. J. Blyth, C. G. Smith, J. S. Wark, M. H. Key, K. Burnett, and M. Nakai, Phys. Rev. A **53**, R31 (1996).
[21] A. L'Huillier (private communication).